Gao *et al. J Wireless Com Network* (2022) 2022:12
https://doi.org/10.1186/s13638-022-02093-8

EURASIP Journal on Wireless Communications and Networking

RESEARCH Open Access

Throughput fairness in cognitive backscatter networks with residual hardware impairments and a nonlinear EH model

Xiaona Gao, Liqin Shi* and Guangyue Lu

*Correspondence:
liqinshi@hotmail.com
Shaanxi Key Laboratory of Information Communication Network and Security, Xi'an University of Posts and Telecommunications, Xi'an 710121, China

Abstract

This paper is to design a throughput fairness-aware resource allocation scheme for a cognitive backscatter network (CBN), where multiple backscatter devices (BDs) take turns to modulate information on the primary signals and backscatter the modulated signals to a cooperative receiver, while harvesting energy to sustain their operations. The nonlinear energy harvesting circuits at the BDs and the residual hardware impairments at the transceivers are considered to better reflect the properties of the practical energy harvesters and transceivers, respectively. To ensure the throughput fairness among BDs, we formulate an optimization problem to maximize the minimum throughput of BDs by jointly optimizing the transmit power of the primary transmitter, the backscattering time and reflection coefficient for each BD, subject to the primary user's quality of service and BDs' energy-causality constraints. We introduce the variable slack and decoupling methods to transform the formulated non-convex problem, and propose an iterative algorithm based on the block coordinate descent technique to solve the transformed problem. We also investigate a special CBN with a single BD and derive the optimal solution in the closed form to maximize the BD's throughput. Numerical results validate the quick convergence of the proposed iterative algorithm and that the proposed scheme ensures much fairness than the existing schemes.

Keywords: Cognitive backscatter network, Energy harvesting, Hardware impairments, Fairness, Convex optimization

1 Introduction

Internet of Things (IoT) is a breakthrough application for wireless communication systems. The ultimate goal of IoT is to make everything (human being, machine and things) achieve ubiquitous connectivity, which requires a large number of spectrum resources [1]. Cognitive radio (CR) enables the IoT nodes to share spectrum with primary users while ensuring that the interference from the IoT nodes does not exceed a predefined threshold, and thus improves spectral efficiency [2, 3]. However, in conventional CR networks, the IoT nodes realize information transmissions by active radios that require power-hungry radio frequency (RF) components, such as mixers, oscillators and analog-digital converters (ADC), leading to a high power consumption and greatly reducing the

operation time of IoT nodes [4, 5]. This issue poses another key challenge for the deployment of massive energy-constrained IoT devices.

Recently, backscatter communication has gained tremendous momentum due to its ability of realizing extra-low-power or even battery-free information transmission. The key idea of backscatter communications is to allow IoT devices, also called backscatter devices (BDs) in this paper, to modulate their information bits over the incident RF signals by adjusting the antenna impedances and to reflect the modulated signals to the associated receivers, while harvesting energy to support their circuit operations [6]. Backscatter communications can be classified into three types, i.e., monostatic backscatter communication system, bistatic backscatter communication system, and ambient backscatter communication (AmBC) system. The monostatic backscatter communication system and bistatic backscatter communication system require dedicated RF sources to generate carrier wave signals, leading to an extra cost. On the contrary, the AmBC system leverages the existing RF signals (e.g., WiFi, Cellular signals), which eliminates the need for the deployment of dedicated RF sources and enjoys a low cost. Meanwhile, we note that in CR, the primary signals can be the existing RF signals required by AmBC. This offers an opportunity to integrate AmBC into CR seamlessly and yields a cognitive backscatter network (CBN) for IoT [7].

The authors of [8] considered a CBN with single user, and maximized the ergodic capacity of a BD by jointly optimizing the primary user's transmit power and the BD's reflection coefficient. In [9], the authors extended the single user scenario in [8] to the multi-user CBN where non-orthogonal multiple access (NOMA) technology is applied to improve the spectral efficiency, and jointly optimized primary user's transmit power and BDs' reflection coefficients to maximize the sum-rate of BDs. In [10], the hybrid backscatter-active transmission was considered and a resource allocation scheme was developed to maximize the overall throughput of IoT devices by balancing the time for backscatter transmission and active transmission. In [11], the authors formulated a joint computation offloading and radio resource allocation problem to minimize the total energy consumption of IoT nodes for multi-access edge computing-based backscatter communication networks. In [12], a joint design for time scheduling, reflection coefficient of BDs together with the transmit power allocation of primary user was proposed in full-duplex-enabled CBN to maximize the throughput of backscatter system, while guaranteeing the minimum rate requirements of the primary system. The authors of [13] maximized the energy efficiency of a CBN with multiple BDs by jointly optimizing the PT transmission power and the BDs' backscatter coefficients and time slot durations for both the parasitic and commensal cognitive redio cases. In [14], the authors investigated the optimal tradeoff between the energy harvesting and backscatter modes, and the optimal reflection coefficient of BD to maximize the throughput of IoT node. Additionally, in [15], the throughput maximization problems for BDs were studied under the premise of the primary user's throughput requirement and BDs' energy-casuality constraints in single- and multi-user CBNs, respectively.

We note that the works mentioned above [8–15] have two limitations. On the one hand, these works assumed an ideal hardware for all active transceivers. However in practice, the hardware impairments (HWIs) exist in RF front ends of active transceivers due to the non-ideal characteristics of electronic circuit, which includes the nonlinearity

of high-power-amplifier (HPA) and the phase noise caused by oscillators [16, 17]. The authors of [18–20] consider the realistic assumptions of HWIs in backscatter communication networks, however, they emphasis on the reliability and the security analysis, and the resource allocation has not been exploited. On the other hand, the linear power conversion efficiency was considered, which does not agree with the fact that the property of practical energy harvesting (EH) circuits is non-linear [21]. The authors in [22] proposed a max–min energy efficiency-based robust resource allocation scheme to maximize the energy efficiency and guarantee the fairness for secure wireless-powered backscatter communication networks under a non-linear EH model. However, the HWIs of the transceivers was ignored. It is worth noting that the existing resource allocation problems under the above ideal assumptions do not match the practical scenarios well and this may lead to resource allocation mismatches. Accordingly, both the problem formulation and its solution need to be revisited.

Inspired by this, in this paper, we formulate a max–min throughput problem for a CBN with multiples BDs while considering the HWIs and a non-linear energy harvesting model, and propose an iterative algorithm to solve it. Our main contributions are listed as follows:

(1) A max–min throughput problem is formulated to ensure fairness among all BDs. To be specific, the minimum throughput of BDs is maximized by jointly optimizing the transmit power of primary transmitter, and the backscattering time and reflection coefficient of each BD, subject to the quality of service (QoS) constraint of primary user and energy-causality constraints of BDs. Please note that in our formulated problem, the practical nonlinear EH model at BDs and HWIs at active transceivers are taken into account, which increases the complexity at optimization stage since the EH function is fractional and the existence of HWIs introduce an additional component to the logarithm objective function with fractional structure. The formulated problem happens to be non-convex, and thus, there is no systematic or computationally-efficient approach to solve it directly.
(2) To solve the non-convex problem, we adopt the following three steps. First, we introduce a slack variable to transform the objective function into a linear one. Second, we determine the optimal transmit power to decouple it from the optimization problem. Third, we propose an iterative algorithm based on the block coordinate descent (BCD) technique, and obtain the sub-optimal solutions for the backscattering time and reflection coefficient of each BD. Besides, we study the special scenario only with a single BD, and derive the closed-form expressions for the optimal time and reflection coefficient.
(3) Simulation results validate the following two results. First, the convergence value of the proposed iterative algorithm is almost similar to the optimal value obtained by the exhaustive search. Second, it is found that the proposed max–min resource allocation scheme is more capable of guaranteeing fairness among BDs, compared with the sum throughput maximization scheme.

The rest of this paper is organized as follows. Section 2 introduces the system model for the general CBN with multi-BD. In Sect. 3, the problem to maximize the minimum

throughput of BDs is formulated, which considers the joint optimization of the transmit power of primary user, the backscattering time and reflection coefficients of BDs. In Sect. 4, we analyze the optimization problem and propose an iterative algorithm to solve it for the resource allocation in multi-BD CBN. Section 5 studies the solution of the optimization problem in CBN with a single BD. In Sect. 6, the performance of the proposed scheme is evaluated by numerical simulations. Section 7 concludes this paper.

2 System model

As depicted in Fig. 1, we consider a cognitive backscatter network with a primary transmitter (PT), a cooperative receiver (C-Rx) and K BDs. The transmission from PT to C-Rx forms the direct link, and PT to kth BD then to C-Rx forms the backscatter link, for $k = 1, \ldots, K$. The PT transmits RF signals to C-Rx by active transmission Each BD is equipped with the backscatter module and energy harvesting circuit so that BD can backscatter information to C-Rx and can harvest energy to power its circuit. C-Rx is designed to recover the signal from the PT as well as the BDs.

The block fading channel is considered in this paper. This means that the channel coefficient remains consistent within one time block and may be changed from one to another. Denote g, h_{1k} and h_{2k} as the channel coefficient of the direct link, the PT to kth BD link and the kth BD to C-Rx link, respectively. In order to obtain the performance bound, we assume perfect channel state information (CSI) for all links.

An entire time block is divided into K slots, i.e.,$\tau_1, \tau_2, \ldots, \tau_K$, followed by the time division multiple access (TDMA) protocol. PT broadcasts RF signals in an entire block, while the K BDs take turn to operate in the backscatter communication mode. Particularly in τ_K, the kth BD utilizes the RF signals to backscatter information to C-Rx, and the non-backscattering BDs operate in the energy harvesting mode.

Let s denote the transmitted signal by PT and satisfy $\mathbb{E}\left[|s|^2\right] = 1$, where $\mathbb{E}[.]$ is the statistical expectation. As shown in Fig. 2, the received signals at the kth BD in τ_k can be expressed as

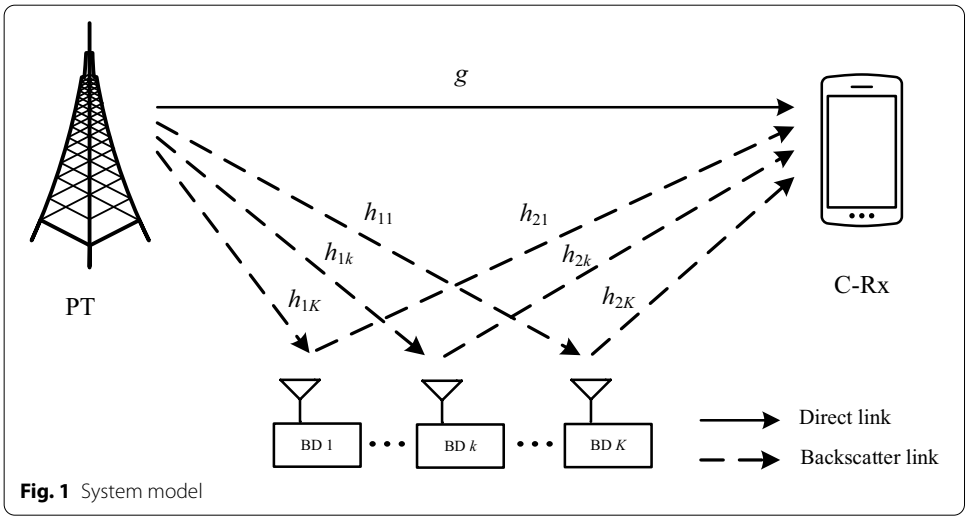

Fig. 1 System model

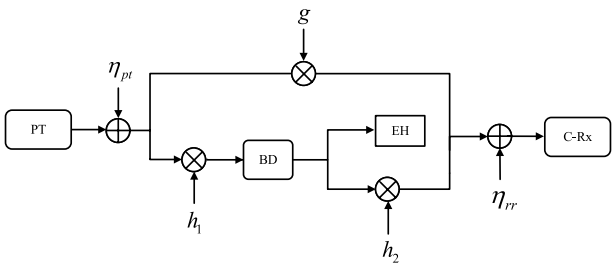

Fig. 2 Block diagram of transmission link with HIs

$$y_{\mathrm{ST},k} = h_{1k}\sqrt{P}\left(s + \eta_{\mathrm{pt}}\right), \tag{1}$$

where P is the transmit power of PT; $\eta_{\mathrm{pt}} \sim \mathrm{CN}\left(0, \kappa_{\mathrm{pt}}^2\right)$ represents the hardware distortion caused by the PT's RF front ends [16, 23], and the parameter κ_{pt} reflects the level of HWIs; $\sqrt{P}h_{1k}\eta_{\mathrm{pt}}$ follows a Gaussian distribution with zero mean and variance $\kappa_{\mathrm{pt}}^2 P\left|h_{1k}\right|^2$. Notice that the power of thermal noise is very small and can be ignored at BDs due to only the passive components included and little signal processing operation involved in its circuit [8, 12, 24].

In τ_k, the kth BD operates in the backscatter communication mode, and splits the received signal into two parts by adjusting the reflection coefficient α_k: $\sqrt{1-\alpha_k}y_{\mathrm{ST},k}$ for energy harvesting, $\sqrt{\alpha_k}y_{\mathrm{ST},k}$ for information transmitting. To better reflect the amount of the harvested energy at the kth BD, the nonlinear EH model proposed in [25] is considered. Therefore, the total harvested energy of the kth BD can be calculated by

$$E_k^h(\alpha_k, \tau_k, P) = \Psi(P_{k,b}^{\mathrm{in}})\tau_k + \Psi(P_{k,h}^{\mathrm{in}})\sum_{i=1}^{k-1}\tau_i. \tag{2}$$

In Eq. (2), the first term $\Psi(P_{k,b}^{\mathrm{in}})\tau_k$ denotes the harvested energy of the kth BD during its backscatter time, where $P_{k,b}^{\mathrm{in}} = P(1-\alpha_k)\left|h_{1k}\right|^2\left(1+\kappa_{\mathrm{pt}}^2\right)$; The second term $\Psi(P_{k,h}^{\mathrm{in}})\sum_{i=1}^{k-1}\tau_i$ represents the harvested energy of the kth BD during the slots $\tau_i, (i = 1, 2, \ldots, k-1)$, where $P_{k,h}^{\mathrm{in}} = P\left|h_{1k}\right|^2\left(1+\kappa_{\mathrm{pt}}^2\right)$; $\Psi(x) = \frac{ax+b}{x+c} - \frac{b}{c}$, is the nonlinear EH mode where x denotes the input power and the correlation coefficients a, b, c can be obtained by fitting curves.

During τ_k, the received signal at C-Rx is given by

$$y_R = \underbrace{g\sqrt{P}\left(s + \eta_{\mathrm{pt}}\right)}_{\text{the first term}} + \underbrace{h_{2k}\sqrt{\alpha_k}y_{\mathrm{ST},k}x_k}_{\text{the scond term}} + \eta_{r,k} + n_{\mathrm{rr}}, \tag{3}$$

where the first term is the signal of the direct link and the second term is the kth BD's backscatter signal, n_{rr} is the additive white Gaussian noise with zero mean and variance of σ_2; x_k with unit power is the signal from the kth BD; $\eta_{r,k}$ is the distorted noise caused by the C-Rx's RF front ends. Note that $\eta_{r,k}$ consists of two parts: η_{r1} and $\eta_{r2,k}$, where $\eta_{r1} \sim \mathrm{CN}\left(0, P\left|g\right|^2\kappa_{\mathrm{rr}}^2\right)$ and $\eta_{r2,k} \sim \mathrm{CN}\left(0, \alpha_k P\left|h_{1k}\right|^2\left|h_{2k}\right|^2\kappa_{\mathrm{rr}}^2\right)$. Hereby, the parameter κ_{rr} reflects the level of HWIs at C-Rx. The multiplicative part $\sqrt{P}g\eta_{\mathrm{pt}}$ follows the Gaussian distribution with zero mean and variance $\kappa_{\mathrm{pt}}^2\left|g\right|^2 P$.

Assume that successive interference cancellation (SIC) technology is employed at C-Rx to decode the received signals. The primary signals can be viewed as a fading channel for the backscatter signals which is modulated on the primary signals. In order to achieve coherent detection, C-Rx has to decode the primary signal first [26]. Specifically, the C-Rx firstly decodes the primary signals and then subtracts it to recover the backscatter signals. Thus the signal-interference-noise-ratio (SINR) to decode the primary signal can be obtain from the following Eq. (4) as

$$\gamma_k^{(1)}(\alpha_k, P) = \frac{P|g|^2}{P|g|^2\kappa_A^2 + \alpha_k P|h_{1k}||h_{2k}|^2(1+\kappa_A^2) + \sigma^2}, \tag{4}$$

where $\kappa_A^2 = \kappa_{\text{pt}}^2 + \kappa_{\text{rr}}^2$.

Accordingly, the SINR to decode the kth BD's backscatter signal with imperfect SIC can be written as

$$\gamma_k^{(2)}(\alpha_k, P) = \frac{\alpha_k P|h_1|^2|h_2|^2}{\xi P|g|^2(1+\kappa_A^2) + \alpha_k P|h_{1k}||h_{2k}|^2\kappa_A^2 + \sigma^2}, \tag{5}$$

where $0 \le \xi \le 1$ is the interference residual factor which quantifies the level of residual interference. Particularly, $\xi = 0$ indicates the perfect SIC and the other values of ξ represent imperfect SIC at the process of recovering backscatter signal [27].

According to the Shannon capacity formula, the achievable throughput of kth BD can be calculated by

$$R_k(\alpha_k, \tau_k, P) = \tau_k W \log_2\left(1 + \Gamma\gamma_k^{(2)}\right), \tag{6}$$

where Γ denotes the performance gap caused by the simple modulation of BDs [28].

3 Problem formulation

In order to guarantee the communication quality fairness, we maximize the minimum throughput among all BDs via jointly optimizing the PT's transmit power, BDs' backscattering time and reflection coefficients while satisfying the QoS of primary user and the energy causality constraints of BDs. Therefore, the optimization problem can be expressed by

$$\begin{aligned}
&\mathbf{P0}: \max_{P,\alpha_k,\tau_k} \min_k R_k \\
&\text{s.t. C1: } 0 \le \alpha_k \le 1, \forall k \\
&\quad \text{C2: } \sum_{i=1}^{K} \tau_i \le 1, \forall k \\
&\quad \text{C3: } \gamma_k^{(1)} \ge \gamma_{\text{th}}, \forall k \\
&\quad \text{C4: } E_k^h \ge P_c\tau_k, \forall k \\
&\quad \text{C5: } 0 \le P \le P_{\max},
\end{aligned} \tag{7}$$

where P_c denotes the minimum circuit consumption for all BDs; γ_{th} denotes the minimum threshold for decoding the primary signal.

In **P0**, C1 and C2 are the practical constraints of backscattering time and reflection coefficients; C3 ensures the QoS for the communication of primary user; C4 maintains

the energy-casuality constraints valid, i.e., the harvested energy is sufficient to cover the power consumption for each BD; C5 considers the transmit power is less than the maximum transmit power $P_{\max}$.

It can be observed that the formulated problem is non-convex and difficult to solve, due to the following two reasons: (1) The objective function is a logarithm function with the fractional form where both numerator and denominator have coupled variables $\alpha_k * P$; (2) The variables α_k, τ_k and P are coupled in C3 and C4. Thus the traditional convex optimization methods cannot be applied directly to solve this problem.

4 Resource allocation in multi-BD CBN

In order to solve **P0**, we adopt the following steps. First, we introduce a slack variable to transform the complex objective function into a affine function. And next, we determine the optimal value of P and decouple it from other optimization variables. Finally, we propose an iterative algorithm to solve the transformed problem based on the block coordinate descent (BCD) technique.

By introducing the slack variable Q, the problem **P0** is converted to

$$\begin{aligned} \mathbf{P1}: & \max_{Q,P,\alpha_k,\tau_k} \ Q \\ \text{s.t. } & \text{C1} \sim \text{C5}, \\ & \text{C6: } R_k^{\min} \geq Q, \ \forall k, \end{aligned} \tag{8}$$

where $R_k^{\min}$ in C6 denotes the minimum throughput of the multi-BD. In addition, C6 ensures the QoS of communication for each BD.

Theorem 1 *The optimal transmit Power is $P_{\max}$, i.e., $P^* = P_{\max}$, where " * " represents the optimal solution.*

Proof Dividing both numerator and denominator by P, one we can see that the Eqs. (3), (4) and (5) are increasing functions with respect to the optimization variable P. One can also see from Eq. (2), the harvested energy of the BDs increases with P. Based on the above description, we conclude that the probability to satisfy constraints C3–C6 increases with P. Combining the above conclusion with the C5, it is not hard to know $P^* = P_{\max}$, where * denotes the optimal value. Theorem 1 is proved. □

Substituting $P_{\max}$ into the problem **P1**, we can simplify **P2** as

$$\begin{aligned} \mathbf{P2}: & \max_{Q,\alpha_k,\tau_k} \ Q \\ \text{s.t. } & \text{C1}: 0 \leq \alpha_k \leq 1, \forall k \\ & \text{C2}: \sum_{i=1}^{K} \tau_i \leq 1, \forall k \\ & \text{C3-1}: \gamma_k^{(1)}(\alpha_k, \tau_k, P_{\max}) \geq \gamma_{\text{th}}, \forall k \\ & \text{C4-1}: E_k^h(\alpha_k, \tau_k, P_{\max}) \geq P_c \tau_k, \forall k \\ & \text{C6-1}: R_k^{\min}(\alpha_k, \tau_k, P_{\max}) \geq Q, \forall k. \end{aligned} \tag{9}$$

Despite the problem **P2** reduces one optimization variable compared with **P1**, it is still non-convex because of the coupled optimization variables α_k and τ_k. To cope with this,

we propose a BCD-based iterative algorithm [29]. In particular, the problem **P2** is decoupled into two convex subproblems, i.e., optimizing the backscattering time τ_k for a given reflection coefficient α_k and optimizing the α_k for a fixed τ_k.

First, for a given reflection coefficient $\alpha_k^{\{l\}}$, we can obtain the backscattering time by solving the following linear programming problem in lth iteration, given as

$$\begin{aligned}
\mathbf{P3}: &\max_{Q,\tau_k} \quad Q \\
&\mathrm{C2}: \sum_{i=1}^{K} \tau_i \le 1, \forall k \\
&\mathrm{C3\text{-}2}: \gamma_k^{(1)}\left(\alpha_k^{\{l\}}, P_{\max}\right) \ge \gamma_{\mathrm{th}}, \forall k \\
&\mathrm{C4\text{-}2}: E_k^h\left(\alpha_k^{\{l\}}, \tau_k, P_{\max}\right) \ge P_c \tau_k, \forall k \\
&\mathrm{C6\text{-}2}: R_k^{\min}\left(\alpha_k^{\{l\}}, \tau_k, P_{\max}\right) \ge Q, \forall k.
\end{aligned} \tag{10}$$

Second, for a given backscattering time $\tau_k^{\{l\}}$, the reflection coefficient can be obtained by solving the following problem in lth iteration, i.e.,

$$\begin{aligned}
\mathbf{P4}: &\max_{Q,\alpha_k} \quad Q \\
\text{s.t. } &\mathrm{C1}: 0 \le \alpha_k \le 1, \forall k \\
&\mathrm{C3\text{-}3}: \gamma_k^{(1)}(\alpha_k, P_{\max}) \ge \gamma_{\mathrm{th}}, \forall k \\
&\mathrm{C4\text{-}3}: E_k^h\left(\tau_k^{\{l\}}, \alpha_k, P_{\max}\right) \ge P_c \tau_k, \forall k \\
&\mathrm{C6\text{-}3}: R_k^{\min}\left(\tau_k^{\{l\}}, \alpha_k, P_{\max}\right) \ge Q, \forall k.
\end{aligned} \tag{11}$$

P4 is a convex problem and the detailed proof can be found in "Appendix". Therefore, **P4** can be efficiently solved by CVX [30].

Based on the above analysis, we propose a BCD-based iterative algorithm to solve **P2**, as summarized in Algorithm 1.

Algorithm 1 BCD-based algorithm for solving problem $\mathbf{P2}$

1: Initialize the refection coefficient $\alpha_k^{\{0\}}, \forall k$; Set the maximum number of iteration as $L_{\max}$, the convergence precision as δ; Let l=0;
2: **Repeat**
3: For given $\alpha_k^{\{l\}}$, solve the problem $\mathbf{P3}$ to obtain the optimal $\tau_k^{\{l+1\}}$.
4: For given $\tau_k^{\{l+1\}}$, solve the problem $\mathbf{P4}$ to obtain the optimal $\alpha_k^{\{l+1\}}$ and $Q^{\{l+1\}}$.
5: **Until** $Q^{\{l+1\}} - Q^{\{l\}} \le \delta$ is met or $l = L_{\max}$.
6: **Return** the optimal resource allocation solution of Problem $\mathbf{P2}$ with $\alpha_k^{\{*\}} = \alpha_k^{\{l\}}$, $\tau_k^{\{*\}} = \tau_k^{\{l\}}$, $\forall k$ and $Q^{\{*\}} = Q^{\{l\}}$.

The convergence of Algorithm 1 is guaranteed because the convex problems **P3** and **P4** in each iteration can be solved by CVX [31]. Assume that the interior point method is adopting to solve the two subproblems and the number of convergence is N_c. The computational complexity of **P3** and **P4** are $O\left(\sqrt{(m)}\log(m)\right)$, $O\left(\sqrt{(n)}\log(n)\right)$ where m and n represent the number of constraints respectively [32, 33]. Therefore, the computational complexity of Algorithm 1 is polynomial, i.e., $N_c O\left(\sqrt{mn}\log(m)\log(n)\right)$ by multiplying the computational complexity solving the convex problems **P3** and **P4**.

5 Resource allocation in single-BD CBN

To obtain the valuable analytical results, we consider the single-BD CBN, i.e., $K = 1$, and discuss the resource allocation scheme in this section. For the single-BD scenario, there is no need to consider the backscattering time allocation. Therefore, the resource allocation problem for the single-BD CBN can be written as

$$\begin{aligned} \mathbf{P5}: & \max_{P,\alpha} R \\ \text{s.t. } & \mathrm{C1}^{'}: 0 \le \alpha \le 1 \\ & \mathrm{C2}^{'}: \gamma^{(1)} \ge \gamma_{\mathrm{th}} \\ & \mathrm{C3}^{'}: E(\alpha, P) \ge P_c \\ & \mathrm{C4}^{'}: 0 \le P \le P_{\max}. \end{aligned} \tag{12}$$

P5 is non-convex due to the existing of coupled variables α and P in the objective function and the constraint $\mathrm{C3}^{'}$. Nevertheless, one observation from the objective function is that, the left-hand side of constraints $\mathrm{C2}^{'}$ and $\mathrm{C3}^{'}$ all increase with P. Taking $\mathrm{C}_5^{'}$ into account, the optimal transmit power can be determined as $P_{\max}$, which is consistent with Theorem 1. Besides, the optimal value of α can be obtained by Lemma 1.

Lemma 1 *The maximum feasible* α *is*

$$\alpha_m = \left\{ \min \left[1 - \frac{cP_c}{P_{\max}\left|h_1\right|^2\left(1+{\kappa_{\mathrm{A}}}^2\right)(ac-b-cP_c)}, \frac{\left|g\right|^2 - \gamma_{\mathrm{th}}\left(\left|g\right|^2{\kappa_{\mathrm{A}}}^2 + \sigma_0^2\right)}{\gamma_{\mathrm{th}}\left|h_1\right|^2\left|h_2\right|^2\left(1+{\kappa_{\mathrm{A}}}^2\right)} \right] \right\}^+ \tag{13}$$

where $\sigma_0^2 = \frac{\sigma^2}{P_{\max}}$ and $\{x\}^+$ *represents* $\max\{0, x\}$.

Proof Given the optimal value of transmit power $P_{\max}$, we can obtain the low bound of α in constraint $\mathrm{C2}^{'}$, which can be derived by

$$\alpha_1 \le \frac{P_{\max}\left|g\right|^2 - \gamma_{\mathrm{th}}\left(P_{\max}\left|g\right|^2{\kappa_{\mathrm{A}}}^2 + \sigma^2\right)}{\gamma_{\mathrm{th}}P_{\max}\left|h_1\right|^2\left|h_2\right|^2\left(1+{\kappa_{\mathrm{A}}}^2\right)}. \tag{14}$$

Similarly, the low bound value of α in constraint $\mathrm{C3}^{'}$ can be obtained by

$$\alpha_2 \le 1 - \frac{cP_c}{P_{\max}\left|h_1\right|^2\left(1+{\kappa_{\mathrm{A}}}^2\right)(ac-b-cP_c)}. \tag{15}$$

Combining the above analysis with the constraint $\mathrm{C1}^{'}$, the largest α in feasible region is given by $\max\{0, \min\{\alpha_1, \alpha_2\}\}$. *Lemma*1 is proved.

Theorem 2 *The optimal solution of* **P5** *is given by*

$$\begin{cases} \alpha^* = \alpha_m \\ P^* = P_{\max} \end{cases} \tag{16}$$

Proof In **P5**, we can observe that the objective function monotonically increases with P for any given feasible α. In order to maximize the throughput, the optimal P should choose the maximum value $P_{\max}$, i.e., $P^* = P_{\max}$. It also can be seen from **P5** that the throughput expression is also a growth function with α for any given feasible P. Thus the maximum throughput is obtained at the largest value of reflection coefficient, i.e., α_m, which is verifiably feasible when $P^* = P_{\max}$ in *Lemma 1*. Based on the above analysis, the values of optimization variables are same as Theorem 2. □

Theorem 2 provides an analytical solution for **P5** and reveals some insights for the considered single-BD scenario. For example, PT adopts the maximum power $P_{\max}$ can improve the throughput performance of BD. And for the energy causality constraint and the primary user's QoS constraint, higher the P, higher is the probability to satisfy the constraints.

6 Results and discussion

In this section, we conduct several simulation experiments to analyze the performance of BDs in CBN. Assume that all the involved channels feature Rayleigh fading with unit variance as small-scale fading and distance exponential fading as large-scale fading. Thus the channel gains can be modeled by $|g|^2 d_0^{-3}$, $|h_{1k}|^2 d_{1k}^{-3}$ and $|h_{2k}|^2 d_{2k}^{-3}$, where d_0 and d_{1k} are the distance from PT to IR and kth BD, and d_{2k} is the distance from kth BD to IR respectively. We set $d_0 = 7$ m, $d_{11} = 2.5$ m, $d_{12} = 4$ m and $d_{21} = 3.5$ m, $d_{22} = 3$ m, respectively. For the nonlinear EH model, we set the correlation parameters $a = 2.463$, $b = 1.735$, $c = 0.826$. In addition, we also assume the same level of HWIs exists at the RF front ends as $\kappa = \kappa_{\text{pt}} = \kappa_{\text{rr}} = 0.1$. The other parameter settings are as shown in Table 1.

Figure 3 depicts the convergence performance of the proposed resource allocation scheme, i.e., Algorithm 1. As shown in this figure, the max–min throughout by proposed algorithm converges closely to the optimal result by exhaustive search method within 10 iterations, which indicates the well convergence performance of the proposed iterative algorithm. Moreover, the max–min throughput by Algorithm 1 increases with the increasing optimal transmit power since there is more energy for BDs to reflect signals.

The max–min throughput based on the proposed resource allocation scheme versus the optimal transmit power is depicted in Fig. 4. As in the theoretical analysis, the max–min throughput increases with the optimal transmit power $P_{\max}$. Additionally, the impact of SINR threshold on the max–min throughput also can be seen in this figure, where the max–min throughput trends down with increasing SINR threshold of the primary user. For the case of $P_{\max} = 10$ dBm, the max–min throughput for $\gamma_{\text{th}} = 5$ dB is 5.173×10^5 bits, which is increased by 11% and 25% compared with $\gamma_{\text{th}} = 6$ dB and $\gamma_{\text{th}} = 7$ dB respectively. The reason for this is that lower SINR threshold reflects higher interference tolerance. In order to cater for the QoS of primary user, BDs have to reduce the transmit power with increased SINR threshold.

Figure 5 shows the max–min throughput performance versus the minimum power consumption of BDs under different conditions of interference residual factor. The performance curve tends to decline as the minimum power consumption increase. The internal reasons can be drawn that BDs cannot but reducing the reflection coefficient to harvest more energy to meet the energy casuality constraint, however, the throughput

Table 1 Simulation parameter settings

Parameters	Symbols	Value
Bandwidth	W	10 MHz
Noise power	σ_2	−114 dBm
SINR threshold	γ_{th}	3 dB
Path-loss exponent	υ	3
Performance gap	Γ	0.1
Interference residual factor	ξ	0.01

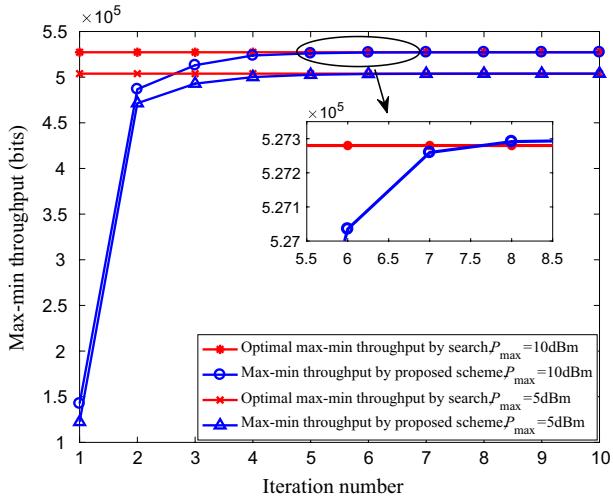

Fig. 3 Convergence performance

function monotonically increases with respect to the reflection coefficient as in Eq. (6). Moreover, we can also see that as the interference residual factor increases, the max–min throughput decreases for any given P_c. For instance, the ξ increases from 0.01 to 0.03, the max–min throughput decreases 26% with $P_c = 0.01$ mW. This is due to that, the interference residual factor quantifies the unremoved interference of primary signals which degrades the performance of BDs.

Figure 6 plots the max–min throughput versus the distance from PT to BD in CBN with a single BD. It can be observed that the increase in distance causes a downward trend in max–min throughput. This is because the channel gain is inversely proportional to distance. BD needs to reduce the reflection coefficient for harvesting sufficient energy to sustain its own circuit with the distance growth, which leads decaying throughput. Besides, we can observe the max–min throughput degrades before the intersection of the curves as κ increases from 0.2 to 0.3, but the contrary is shown after the intersection. This is due to the fact that the HWIs can compensate part of the harvested energy as described by Eq. (2), which improves the performance in higher distance regime.

Take the sum throughput maximization resource allocation scheme as benchmark scheme for comparison. It is important to note that Algorithm 1 also works for the benchmark scheme to obtain the resource allocation management. Figure 7 shows the

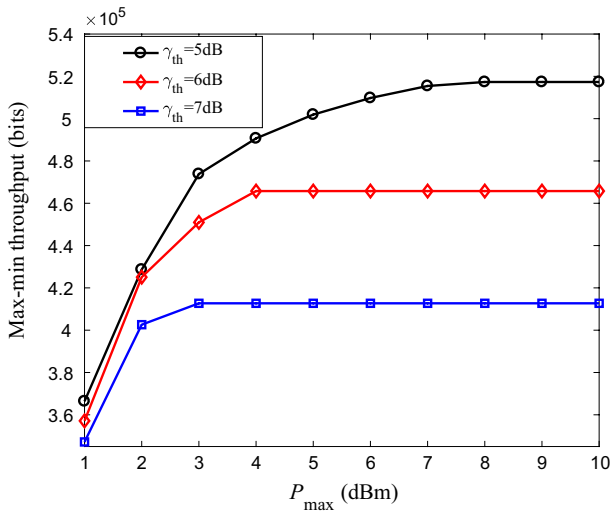

Fig. 4 Max–min throughput (bits) versus the optimal transmit power $P_{\max}$ with different decoding threshold γ_{th} of primary user

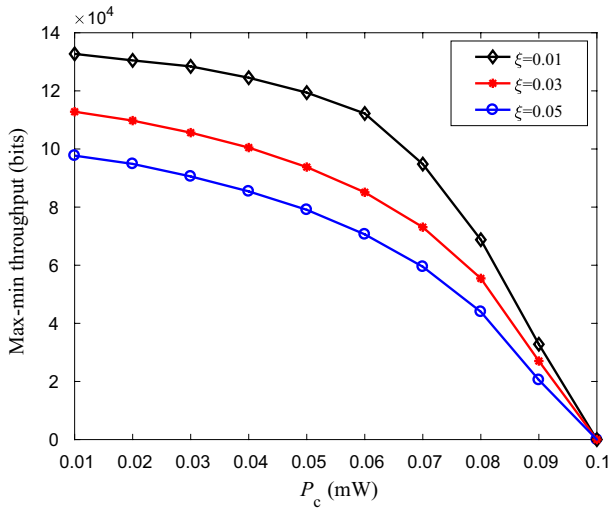

Fig. 5 Max–min throughput (bits) versus the minimum power consumption with different interference residual factor ξ for $P_{\max} = 5$ dB

comparison of the proposed scheme based on max–min criterion with the benchmark scheme. First, we can visualize that the difference of throughput between the best and worst links from the proposed max–min scheme is less than the benchmark scheme whether in the scenarios of two or four BDs. Second, the difference of throughput between the best and worst links from the benchmark has increased nearly threefold as the number of users increases from 2 to 4, which is significantly larger than the difference increase of the proposed max–min scheme. Third, the average throughput of benchmark scheme is slightly outperform than the proposed max–min scheme. This is because, benchmark scheme inclines to the users with good channel status to obtain the

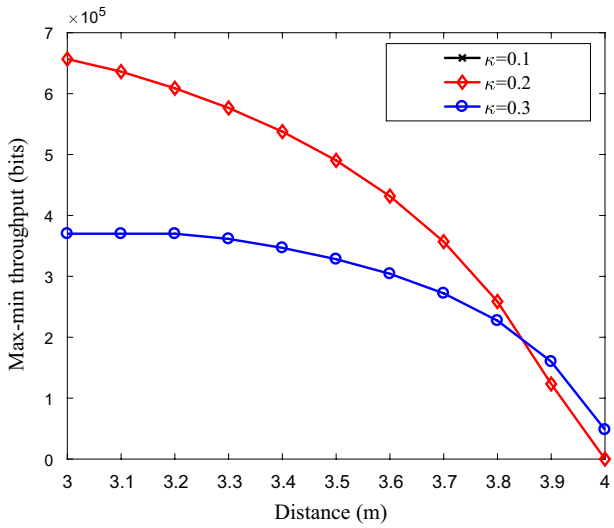

Fig. 6 Max–min throughput (bits) versus the distance of PT-BD with different level of HIs for $P_{\max} = 5$ dBm

maximum of sum throughput, while the proposed scheme maximizes the throughput of user with worst link status to guarantee much fairness of inter-BD. In conclusion, the max–min scheme at the expense of slightly less throughput achieves much fairness.

7 Conclusion

In this paper, we studied the max–min resource allocation scheme considering the non-linear EH model and the existence of HWIs. Specifically, we formulate the joint PT's transmit power, BDs' backscattering time and reflection coefficients optimization problem for maximizing the minimum throughput of BDs, and propose an iterative algorithm based on BCD to solve the optimization problem. In addition, we obtained the closed-form solution of the optimization problem in the special scenario for the CBN

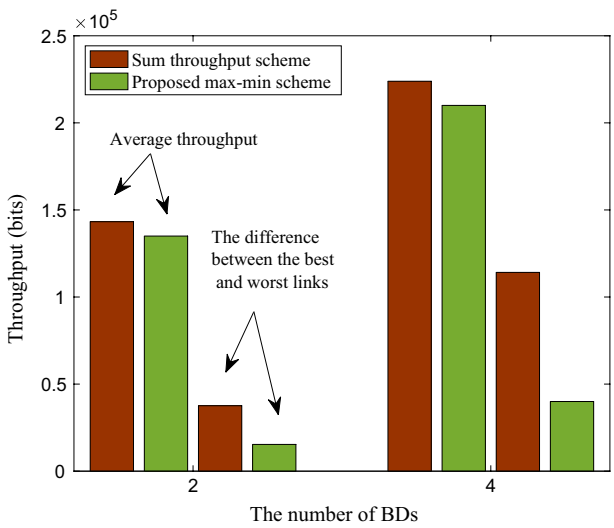

Fig. 7 Comparison of throughput under max–min scheme and sum throughput maximization scheme

with single-BD. Simulation results demonstrated the proposed max–min resource allocation scheme efficiently ensures fairness among BDs and revealed the effect of different relevant parameters like the QoS of primary user, distance from PT to BD, the level of HWIs, etc.

Appendix

In **P4**, the constraint C3-3 can be transformed to a linear constraint as described in Eq. (14). The objective function and constraint C1 are affine. Therefore, we just need to discuss the concavity of the constraints C4-3 and C6-3.

For the constraint C4-3, the second term of the left-hand side is a constant independent of the variables, thus we only discuss the first term marked by $E_k(x)$. Taking the second order derivative of $E_k(x)$ yields

$$\frac{\partial^2 E_k}{\partial x^2} = \frac{(b-ac)\left(\left|h_{1k}\right|^2\left(1+\kappa_B^2\right)P_{\max}\right)^2}{\left((1-\alpha_k)\left|h_{1k}\right|^2\left(1+\kappa_B^2\right)P_{\max}+c\right)^3}, \tag{17}$$

where the positivity and negativity is determined by $b-ac$ and c. According to the non-negativity and saturation properties of nonlinear EH model, the correlations between the parameters in the adopted model are proved in [34] as $b-ac<0$ and $c>0$. Thus $\frac{\partial^2 E_k}{\partial x^2}<0$ and C4-3 is a convex constraint.

For the constraint C6-3, it has the same structure as $H(x)=\log\left(1+\frac{Ax}{Bx+C}\right)$ where the parameters A, B and C are all above zero. Taking the second order derivative of $H(x)$, we can derive

$$\frac{\partial^2 H}{\partial x^2} = -\frac{\left(2ABx+2B^2x+2BC+AC\right)^2 C}{\left[(Ax+Bx+C)(Bx+C)\right]^2 \ln 2}. \tag{18}$$

In Eq. (18), we can visualize that $\frac{\partial^2 H}{\partial x^2}<0$. Thus the left-hand side of C6-3 is a concave function. This means C6-3 is a convex constraint.

From the analyses made above, we can draw the conclusion that **P4** is a convex problem [35].

Abbreviations

CBN: Cognitive backscatter network; BDs: Backscatter devices; C-Rx: Cooperative receiver; HWIs: Hardware impairments; EH: Energy harvesting; IoT: Internet-of-things; QoS: Quality of service; CR: Cognitive radio; ADC: Analog-digital converters; RF: Radio frequency; PT: Primary transmitter; AmBC: Ambient backscatter communication; HPA: High-power-amplifier; TDD: Time-division-multiplexing; CSI: Channel state information; SIC: Successive interference cancellation; BCD: Block coordinate descent.

Acknowledgements

No applicable.

Author's contribution

LS conceived of the study, designed and modeled. XG carried out experiments, participated in the performance analysis and drafted the manuscript. GL participated in the design and helped to draft the manuscript. All authors read and approved the final manuscript.

Author's information
Xiaona Gao received the B.E. degree from Xuchang University, Henan, China, in 2020. She is currently pursuing the the M.S. degree in the Xi'an University of Posts and Telecommunications, Xi'an, China. Her current research interests include wireless communication technology, and ambient backscatter systems.
Liqin Shi received the B.S. degree from Sichuan University, Chengdu, China, in 2015, and the Ph.D. degree from Xidian University, Xi'an, China, in 2020. She was a Joint Ph.D. student with the Department of Electrical and Computer Engineering, Utah State University, Logan, UT, USA, from 2018 to 2019. Since 2020, she has been with the Xi'an University of Posts and Telecommunications, Xi'an, where she is currently an Associate Professor with the Department of Communication and Information Engineering. She has published more than 20 papers in IEEE Transactions on Vehicular Technology and IEEE ICC. Her research interests include wireless energy harvesting and mobile-edge computing. Dr. Shi is also a reviewer of multiple international journals, including the IEEE Journal on Selected Areas in Communications and the IEEE Transactions on Wireless Communications. She has served as a TPC member of IEEE SmartIoT in 2018 and IEEE VTC-FALL in 2019.
Guangyue Lu received the Ph.D. degree from Xidian University, Xi'an, China, in 1999. From September 2004 to August 2006, he was a Guest Researcher with the Signal and Systems Group, Uppsala University, Uppsala, Sweden. Since 2005, he has been a Full Professor with the School of Communications and Information Engineering, Xi'an University of Posts and Telecommunications, Xi'an. He has been the funded by over twenty projects including the National Natural Science Foundation of China, the 863 Program, and Important National Science and Technology Specific Projects. Due to his excellent contributions in education and research, he was awarded by the Program for New Century Excellent Talents in University, Ministry of Education, China, in 2009. He is currently the Vice President of Xi'an University of Posts and Telecommunications, and the Director of the Shaanxi Key Laboratory of Information Communication Network and Security. His research interests include wireless communications, energy harvesting, cognitive radio and cooperative spectrum sensing.

Funding
This work was supported by the Science and Technology Innovation Team of Shaanxi Province for Broadband Wireless and Application under Grant 2017KCT-30-02, the Natural Science Foundation of Shaanxi Province under Grant 2021JQ-713 and the Postgraduate Innovation Fund of Xi'an University of Posts, and Telecommunications under Grant CXJJYL2021064.

Availability of data and materials
Data sharing not applicable to this article as no datasets were generated or analysed during the current study.

Declarations

Competing interests
The authors declare that they have no competing interests.

Received: 2 November 2021 Accepted: 23 January 2022
Published online: 08 February 2022

References

1. F. Rezaei, C. Tellambura, S. Herath, Large-scale wireless-powered networks with backscatter communications: a comprehensive survey. IEEE Open J. Commun. Soc. **1**, 1100–1130 (2020). https://doi.org/10.1109/OJCOMS.2020.3012466
2. A.A. Khan, M.H. Rehmani, A. Rachedi, Cognitive-radio-based internet of things: applications, architectures, spectrum related functionalities, and future research directions. IEEE Wirel. Commun. **24**(3), 17–25 (2017). https://doi.org/10.1109/MWC.2017.1600404
3. Y. Xu, G. Gui, H. Gacanin, F. Adachi, A survey on resource allocation for 5g heterogeneous networks: current research, future trends, and challenges. IEEE Commun. Surv. Tutor. **23**(2), 668–695 (2021). https://doi.org/10.1109/COMST.2021.3059896
4. Y. Ye, L. Shi, X. Chu, G. Lu, On the outage performance of ambient backscatter communications. IEEE Internet Things J. **7**(8), 7265–7278 (2020). https://doi.org/10.1109/JIOT.2020.2984449
5. H. Yang, Y. Ye, X. Chu, S. Sun, Energy efficiency maximization for UAV-enabled hybrid backscatter-harvest-then-transmit communications. IEEE Trans. Wirel. Commun. (2021). https://doi.org/10.1109/TWC.2021.3116509
6. N. Van Huynh, D.T. Hoang, X. Lu, D. Niyato, P. Wang, D.I. Kim, Ambient backscatter communications: a contemporary survey. IEEE Commun. Surv. Tutor. **20**(4), 2889–2922 (2018). https://doi.org/10.1109/COMST.2018.2841964
7. R. Long, Y.-C. Liang, H. Guo, G. Yang, R. Zhang, Symbiotic radio: a new communication paradigm for passive internet of things. IEEE Internet Things J. **7**(2), 1350–1363 (2020). https://doi.org/10.1109/JIOT.2019.2954678
8. X. Kang, Y.-C. Liang, J. Yang, Riding on the primary: a new spectrum sharing paradigm for wireless-powered IoT devices. IEEE Trans. Wirel. Commun. **17**(9), 6335–6347 (2018). https://doi.org/10.1109/TWC.2018.2859389
9. J. Wang, H.-T. Ye, X. Kang, S. Sun, Y.-C. Liang, Cognitive backscatter NOMA networks with multi-slot energy causality. IEEE Commun. Lett. **24**(12), 2854–2858 (2020). https://doi.org/10.1109/LCOMM.2020.3019203
10. Y. Zhuang, X. Li, H. Ji, H. Zhang, V.C.M. Leung, Optimal resource allocation for RF-powered underlay cognitive radio networks with ambient backscatter communication. IEEE Trans. Veh. Technol. **69**(12), 15216–15228 (2020). https://doi.org/10.1109/TVT.2020.3037152
11. Y. Xu, B. Gu, R.Q. Hu, D. Li, H. Zhang, Joint computation offloading and radio resource allocation in MEC-based wireless-powered backscatter communication networks. IEEE Trans. Veh. Technol. **70**(6), 6200–6205 (2021). https://doi.org/10.1109/TVT.2021.3077094

12. S. Xiao, H. Guo, Y.-C. Liang, Resource allocation for full-duplex-enabled cognitive backscatter networks. IEEE Trans. Wirel. Commun. **18**(6), 3222–3235 (2019). https://doi.org/10.1109/TWC.2019.2912203
13. H. Yang, Y. Ye, K. Liang, X. Chu, Energy efficiency maximization for symbiotic radio networks with multiple backscatter devices. IEEE Open J. Commun. Soc. **2**, 1431–1444 (2021). https://doi.org/10.1109/OJCOMS.2021.3090836
14. B. Lyu, C. You, Z. Yang, G. Gui, The optimal control policy for RF-powered backscatter communication networks. IEEE Trans. Veh. Technol. **67**(3), 2804–2808 (2018). https://doi.org/10.1109/TVT.2017.2768667
15. G. Yang, D. Yuan, Y.-C. Liang, R. Zhang, V.C.M. Leung, Optimal resource allocation in full-duplex ambient backscatter communication networks for wireless-powered IoT. IEEE Internet Things J. **6**(2), 2612–2625 (2019). https://doi.org/10.1109/JIOT.2018.2872515
16. Z. Liu, G. Lu, Y. Ye, X. Chu, System outage probability of PS-SWIPT enabled two-way AF relaying with hardware impairments. IEEE Trans. Veh. Technol. **69**(11), 13532–13545 (2020). https://doi.org/10.1109/TVT.2020.3030134
17. E. Costa, M. Midrio, S. Pupolin, Impact of amplifier nonlinearities on OFDM transmission system performance. IEEE Commun. Lett. **3**(2), 37–39 (1999). https://doi.org/10.1109/4234.749355
18. X. Li, M. Zhao, M. Zeng, S. Mumtaz, V.G. Menon, Z. Ding, O.A. Dobre, Hardware impaired ambient backscatter NOMA systems: reliability and security. IEEE Trans. Commun. **69**(4), 2723–2736 (2021). https://doi.org/10.1109/TCOMM.2021.3050503
19. X. Li, Y. Zheng, M.D. Alshehri, L. Hai, V. Balasubramanian, M. Zeng, G. Nie, Cognitive AmBC-NOMA IoV-MTS networks with IQI: reliability and security analysis. IEEE Trans. Intell. Transp. Syst. (2021). https://doi.org/10.1109/TITS.2021.3113995
20. X. Li, M. Zhao, Y. Liu, L. Li, Z. Ding, A. Nallanathan, Secrecy analysis of ambient backscatter NOMA systems under I/Q imbalance. IEEE Trans. Veh. Technol. **69**(10), 12286–12290 (2020). https://doi.org/10.1109/TVT.2020.3006478
21. C.R. Valenta, G.D. Durgin, Harvesting wireless power: Survey of energy-harvester conversion efficiency in far-field, wireless power transfer systems. IEEE Microwave Mag. **15**(4), 108–120 (2014). https://doi.org/10.1109/MMM.2014.2309499
22. Y. Xu, B. Gu, D. Li, Robust energy-efficient optimization for secure wireless-powered backscatter communications with a non-linear EH model. IEEE Commun. Lett. **25**(10), 3209–3213 (2021). https://doi.org/10.1109/LCOMM.2021.3097737
23. S. Solanki, V. Singh, P.K. Upadhyay, Rf energy harvesting in hybrid two-way relaying systems with hardware impairments. IEEE Trans. Veh. Technol. **68**(12), 11792–11805 (2019). https://doi.org/10.1109/TVT.2019.2944248
24. J. Qian, F. Gao, G. Wang, S. Jin, H. Zhu, Noncoherent detections for ambient backscatter system. IEEE Trans. Wirel. Commun. **16**(3), 1412–1422 (2017). https://doi.org/10.1109/TWC.2016.2635654
25. Y. Chen, N. Zhao, M.-S. Alouini, Wireless energy harvesting using signals from multiple fading channels. IEEE Trans. Commun. **65**(11), 5027–5039 (2017). https://doi.org/10.1109/TCOMM.2017.2734665
26. G. Wang, F. Gao, R. Fan, C. Tellambura, Ambient backscatter communication systems: detection and performance analysis. IEEE Trans. Commun. **64**(11), 4836–4846 (2016). https://doi.org/10.1109/TCOMM.2016.2602341
27. L. Luo, Q. Li, J. Cheng, Performance analysis of overlay cognitive NOMA systems with imperfect successive interference cancellation. IEEE Trans. Commun. **68**(8), 4709–4722 (2020). https://doi.org/10.1109/TCOMM.2020.2992471
28. S.H. Kim, D.I. Kim, Hybrid backscatter communication for wireless-powered heterogeneous networks. IEEE Trans. Wirel. Commun. **16**(10), 6557–6570 (2017). https://doi.org/10.1109/TWC.2017.2725829
29. M. Razaviyayn, M. Hong, Z.Q. Luo, J.S. Pang, Parallel successive convex approximation for nonsmooth nonconvex optimization. Advances in neural information processing systems (2014)
30. M. Grant, S. Boyd, CVX: Matlab Software for Disciplined Convex Programming, version 2.1. http://cvxr.com/cvx (2014)
31. M. Razaviyayn, M. Hong, Z.Q. Luo, A unified convergence analysis of block successive minimization methods for nonsmooth optimization. SIAM J. Optim. **23**(2), 1126–1153 (2012)
32. L. Shi, Y. Ye, R.Q. Hu, H. Zhang, Energy efficiency maximization for SWIPT enabled two-way DF relaying. IEEE Signal Process. Lett. **26**(5), 755–759 (2019). https://doi.org/10.1109/LSP.2019.2906463
33. L. Shi, R.Q. Hu, J. Gunther, Y. Ye, H. Zhang, Energy efficiency for RF-powered backscatter networks using HTT protocol. IEEE Trans. Veh. Technol. **69**(11), 13932–13936 (2020). https://doi.org/10.1109/TVT.2020.3014500
34. Y. Ye, L. Shi, X. Chu, G. Lu, Throughput fairness guarantee in wireless powered backscatter communications with HTT. IEEE Wirel. Commun. Lett. **10**(3), 449–453 (2021). https://doi.org/10.1109/LWC.2020.3014740
35. S. Boyd, S.P. Boyd, L. Vandenberghe, *Convex Optimization* (Cambridge University Press, Cambridge, 2004)

Publisher's Note